Eur. Phys. J. B **40**, 415–419 (2004)
DOI: 10.1140/epjb/e2004-00249-y

THE EUROPEAN PHYSICAL JOURNAL B

Observing the lateral confinement of surface state electrons in room temperature stable metallic nanostructures

F. Calleja, J.J. Hinarejos, A.L. Vázquez de Parga, and R. Miranda[a]

Departamento de Física de la Materia Condensada, Instituto Nicolás Cabrera, Universidad Autónoma de Madrid, Cantoblanco, 28049 Madrid, Spain

Received 15 December 2003
Published online 10 August 2004 –

Abstract. The lateral confinement of the surface state electrons of Cu(111) has been studied by Scanning Tunnelling Microscopy and Spectroscopy at low temperature. The confining nanostructures are Cu(111) islands embedded in a semiconducting Cu_3N(111) film which completely isolate them from each other. The standing wave pattern observed reflect the shape of the edge of the islands, i.e. the positions of the confining potential as long as the islands are larger than twice the Fermi wavelength of the surface electrons. The interference pattern in smaller islands is more complex, reflecting the collective behavior of the electrons. When the width of the islands is, at least in one dimension, smaller than the Fermi wavelength, there is a clear shift in the energy of the bottom of the surface band towards the Fermi level. The depopulation of the surface state produced by lateral confinement might have important consequences with respect to the reactivity of these nanostructures.

PACS. 68.37.Ef Scanning tunneling microscopy (including chemistry induced with STM) – 73.20.At Surface states, band structure, electron density of states – 73.22.-f Electronic structure of nanoscale materials: clusters, nanoparticles, nanotubes, and nanocrystals

1 Introduction

The electronic states of metallic nanostructures are different from their bulk (and extended surfaces) counterparts due to quantum confinement and so are their properties. Major changes in the properties of a given material occur in the nanometer range due to quantum confinement. Icosahedral Au nanocrystals 3−5 nm in diameter, for instance, oxidize CO even at 200 K [1] while extended Au surfaces are completely inert towards CO. In Au nanosized crystallites, the lattice constant is smaller, probably as a consequence of the enhanced stress in the Au clusters. Furthermore, not only the ratio surface atoms/"bulk" atoms is extraordinary large in the smallest clusters, but also the surfaces are limited in size. All these facts have consequences regarding the electronic states of these nanocrystallites. In particular, the confinement of the surface state of Au on the limited (111) facets that bind the nanocrystallites might be relevant. It has been found that the energy of the confined states determines structural properties such as the "magic" heights in Pb nanocrystals [2] and the special stability of certain heights in Ag films on metallic substrates [3]. It is, thus, important to determine experimentally the modifications in the electronic structure of nano-objects produced by confinement.

In the following we will concentrate on some effects produced by lateral confinement on the surface states. Most surfaces posses a specific set of electronic states whose wave functions are strongly confined to a narrow region perpendicular to the surface [4,5]. They play an essential role in many surface properties and have been the subject of a detailed scrutiny over the years. Recently, the development of the STM has offered unique opportunities of unveiling the behavior of surface electrons with unprecedented detail, since it maps the Local Density Of States (LDOS) some Å above the surface. Restricting ourselves to the free-electron-like surface states on (111) surfaces of noble metals, the standing waves in electron density resulting from interference of surface state electrons scattering off steps and point defects have been directly visualized [6], their wavelength and energy dispersion, $E(k)$ measured [6], and their Fourier transform employed to get information on the 2D Fermi contour [7] of the surface state electrons. More recently, the lifetime of the surface electrons, which reflects the different interactions (electron-electron, electron-phonon, etc) in solids, was determined as a function of energy and temperature [8].

The changes in the electronic states produced by further confinement of surface electrons in artificial nanostructures have also been explored. These nanostructures, i.e. Fe corrals on Cu(111) [9] or Ag islands on Ag(111) [10] are only stable at low temperatures, i.e. they are destroyed by thermal diffusion upon heating to 300 K. We describe here an alternate method to fabricate nanometer-sized metal islands embedded in a non-metallic overlayer that

[a] e-mail: rodolfo.miranda@uam.es

are stable at 300 K and report on the electronic states of the confined system.

2 Experimental

The experiments have been carried out in an Ultra High Vacuum (UHV) chamber with base pressure in the low 10^{-10} Torr regime. The chamber contains a variable temperature STM microscope, a reverse view Low Energy Electron Diffraction (LEED) optics, and facilities for ion sputtering and evaporation. The Cu(111) surface was cleaned by ion sputtering (1 kV) and annealing to 700 K. The polycrystalline W STM tips were cleaned in situ by means of ion bombardment and field emission, as described elsewhere [11]. All images were recorded in the constant current mode. The *I-V* curves were taken at 65−300 K and numerically differentiated to obtain the *dI/dV* differential tunnelling conductance spectra.

3 Results and discussion

The Shockley surface state of Cu(111) constitutes a quasi-2D nearly-free electron gas with 0.04 electrons per surface atom (i.e. 7×10^{13} electrons cm^{-2}), two orders of magnitude denser than the 2D electron gas at the interface of a semiconductor heterojunction. The mobility, however, is four orders of magnitude smaller than in a high quality semiconductor 2D electron gas. The kind of information of the surface state electrons of an extended surface that can be obtained from STM is illustrated in Figure 1 where we show an STM image of a large terrace of Cu(111) displaying *simultaneously* atomic resolution (i.e. the lattice of the Cu atoms) and the circular quantum mechanical interference pattern (visible as oscillations in the apparent height) due to the surface state electrons scattered by the potential associated to a few points defects in the terrace. In order to get an accurate determination of the 2D Fermi contour (see below), point scatterers are preferred to steps, since in the first case wavevectors from all the Fermi contour contribute to form the standing wave pattern. The decay of the amplitude of the standing waves away from straight steps, on the other hand, is convenient to determine electron lifetimes [8]. The atomic corrugation in the conditions of Figure 1 is 0.2 Å, while the standing wave corrugation is 0.1 Å. Since the sample voltage is only −5 mV, the oscillations correspond to electrons in the surface state right at the Fermi level. The standing waves, thus, show a period of half the Fermi wavelength, i.e. 15 Å. In agreement with previous reports [6], topographic STM images recorded at slightly larger tunnelling gap resistance (not shown) display only the electron interference pattern produced by scattering off step edges and point defects in Cu(111).

The (unfiltered) Fourier transform of this image is reproduced in Figure 2. It shows a map of the k vectors that contribute to the standing wave pattern. Spots reflecting the reciprocal lattice of the Cu(111) surface (originating from the atomic resolution) *and* circles corresponding to the 2D Fermi contour, i.e. the crossing of the Fermi level by the surface state, are seen. The 2D Fermi contour is totally equivalent to the bulk Fermi surface. Accordingly, it dictates the response of the 2D electron gas to any static or dynamic disturbance. The experimental determination of the 2D Fermi contour is important since the electronic instabilities at the surface are connected to its shape and they may lead to the stabilization of Charge Density Waves, Peierls distortions of the lattice, many body effects and other collective phenomena. Most of the 2D Fermi contours reported to date have been obtained from STM images *not* showing simultaneously atomic resolution and standing waves [12]. In that case, any distortion in the image coming from creep in the piezos, thermal drift, etc., results in a distorted shape of the Fermi contour, which might lead to substantial mistakes in the interpretation of the physics behind [13,14]. On the contrary, the Fourier transform of an image such as shown in Figure 1 contains an internal calibration, because the distance separating the lattice spots in the Fourier transform is related to the well known lateral lattice parameter of Cu(111). In this case one can determine with high precision the size of the surface Fermi wave vector, which turns out to be $\mathrm{k}_F = 0.205 \pm 0.02$ Å^{-1}, i.e. a Fermi wavelength of 30 ± 3 Å for Cu(111), in excellent agreement with Angular Resolved Ultraviolet Photoelectron Spectroscopy (ARUPS) measurements [15]. This method, dubbed FT-STM [7], has an energy resolution that depends on the bias voltage and temperature and a momentum resolution that depends on the size of the image and the broadening of the Fermi contour due to the thermal decay of the standing

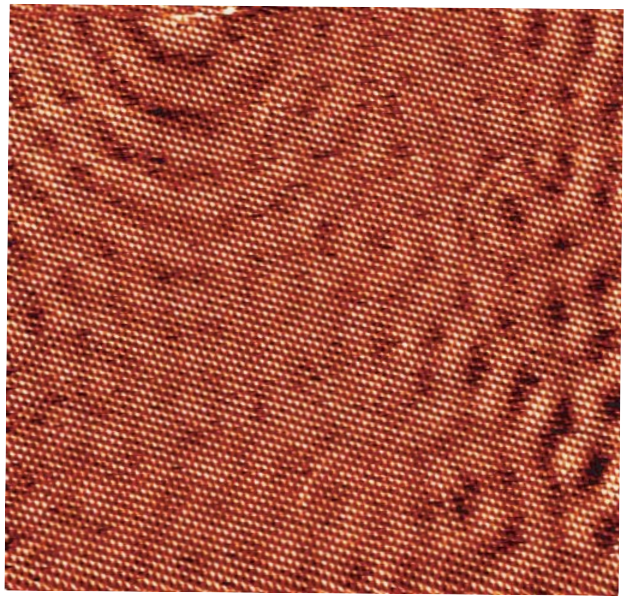

Fig. 1. 20 nm × 20 nm constant current STM topograph of a Cu(111) surface (raw data) displaying both the atomic lattice and the LDOS oscillations. The image has been recorded at 60 K with a sample voltage of −5 mV and a tunnelling resistance of 10 MΩ.

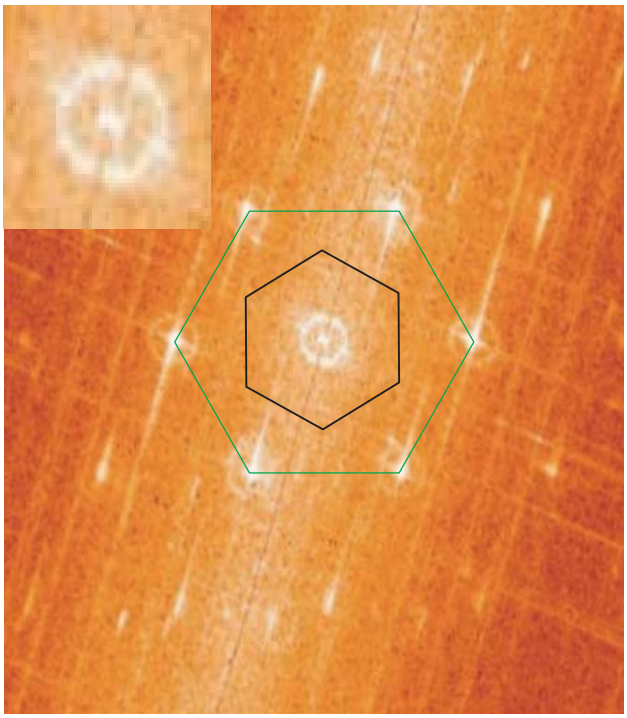

Fig. 2. Unfiltered 2D Fourier transform of the image in Figure 1. The rings detected around the central spot (see inset) and the other lattice spots have twice the radius of the 2D Fermi contour of the surface state. The lines in the power spectrum reflect the residual mechanical vibrations of the experimental setup.

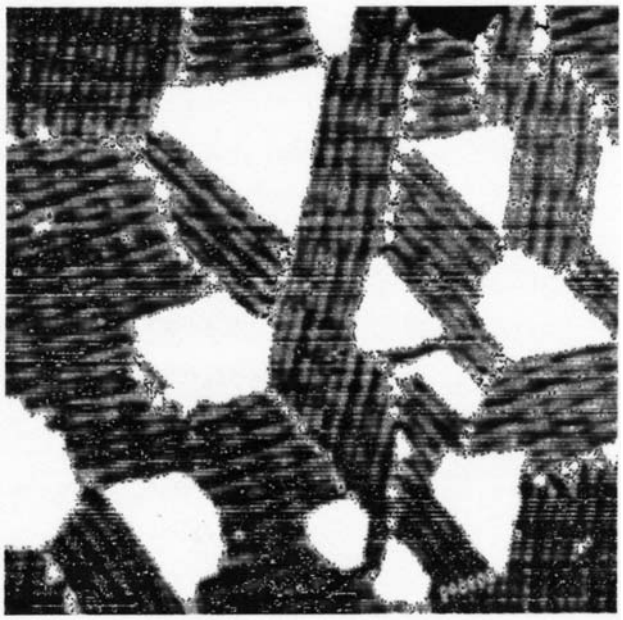

Fig. 3. 50 nm × 50 nm constant current STM image of the surface of a Cu(111) crystal bombarded with 300 eV N^+ ions to a dose of 20 μC and heated to 700 K. The image has been recorded at 300 K with $V_s = -1$ V and a gap resistance of 6.2 GΩ. There are three domains of the reconstructed Cu_3N (111) overlayer.

waves. If both are selected properly it can compete with the best ARUPS data avalaible.

The electrons in the surface state of Cu(111) can be further confined laterally in nanostructures that are stable at room temperature. Partial nitridation of a Cu(111) surface produces Cu(111) islands separated by semiconducting Cu_3N. This was achieved by bombarding the Cu crystal with 200−500 eV N^+ ions to doses of 20−60 μC, followed by heating to 700 K [16]. Bombarding with N^+ at ion doses higher than 200 μC results in N-containing layers, structurally similar to $Cu_3N(111)$ that cover totally the surface. Lowering the dose and carefully adjusting the annealing conditions results in the growth of a N-reconstructed surface layer in which isolated, nanosized Cu (111) islands are embedded, as illustrated in Figure 3. The bright areas of the image are clean Cu(111) patches. The image has been taken at 300 K and the Cu nanoislands are stable at this temperature. The N-containing regions are imaged with an apparent height 1.9 Å below the Cu surface indicating that they have a lower LDOS in an energy region of the order of 1 eV around the Fermi level. Three domains of the N reconstruction aligned with the closed-packed row of the Cu substrate are clearly visible in the same terrace. Higher resolution STM images (not shown here) proof that the Cu atoms in the reconstruction form a distorted (100) surface onto which N atoms form a $c(2 \times 2)$ arrangement [17]. The coincidence mesh of the pseudo (100) $c(2 \times 2)$ overlayer with the underlying (111) surface gives the $(25 \times 7\sqrt{3})$ rectangular unit cell that originates the complex LEED pattern reported previously [18].

For the purpose of this work the most relevant characteristic of the N-reconstructed surface regions is their semiconducting character (to be proven below) that forbids the lateral propagation of the surface-state electrons of Cu. Thus the lateral confinement is provided by the lack of states at the Fermi level and the lattice mismatch. The standing wave pattern observed at low T on one of the Cu(111) patches is shown in Figure 4. The central island has a size of 330 Å × 120 Å. As long as the Cu islands are larger than twice the Fermi wavelength of the surface state, the shape of the standing wave pattern reflects precisely the shape of the island edges, that is, the "quantum box" where the electrons are confined. Standing waves have been detected previously on the same system for Cu islands with the shape of triangles, parallelograms or trapezoids [19]. In that work, the smallest islands were 120 Å wide and the pattern always reproduces faithfully the shape of the edges. Circular quantum corrals of Fe atoms on Cu(111), 140−170 Å in diameter and kept at 4 K were the first artificial structures to show specific patterns of standing waves that reflect the shape of 0 D structures [9]. Islands of Ag on Ag(111) [10] were also observed to display regular standing wave patterns, but these nanostructures are not stable at 300 K, decaying by diffusion of the adatoms that compose them. Interference patterns of surface electrons on room temperature-stable islands of Ni on Cu(111) have been observed recently [20].

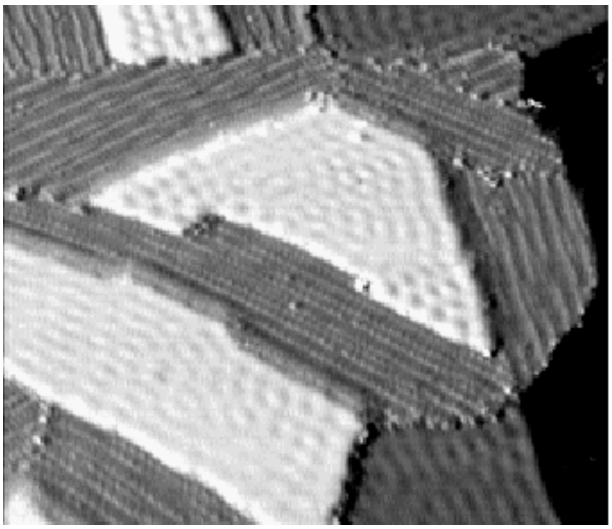

Fig. 4. 50 nm × 43 nm constant current STM image of Cu(111) islands surrounded by the N-induced reconstruction. The sample was bombarded with 500 eV N^+ions to a dose of 15 μC. The image was taken at 65 K, with a sample voltage of $V_s = -12$ mV and a tunnelling resistance of 133 MΩ. A fraction of the derivative has been added to the image to display simultaneously the standing waves on top of the Cu islands and the surface reconstruction in the Cu_3N(111) film.

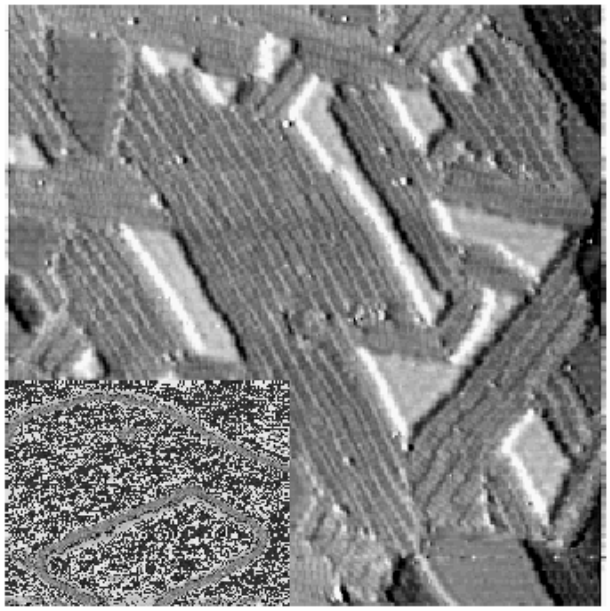

Fig. 5. 50 nm × 50 nm constant current STM image of the surface of a Cu(111) crystal N^+-bombarded and annealed to 700 K. The sample voltage was 0.3 V and the tunnelling resistance, 2.7 GΩ. The bright regions are islands of Cu. The inset shows a 30 nm × 24 nm constant current STM topograph of the standing wave pattern on a trapezoidal Cu(111) island surrounded by a semiconducting Cu_3N layer. The image was taken at 65 K with $V_s = -5$ mV and a gap resistance of 55.5 MΩ.

In that case, however, the intermixing between Ni and Cu jeopardizes the clear assignment of the surface state.

The STM image of Figure 5 taken at 300 K shows a region of the surface with numerous Cu(111) islands of smaller sizes. For example the trapezoidal island at the center left has a size of 38 Å × 126 Å and the triangular island at the center right has a side of 80 Å. The pattern of standing waves observed upon lowering the temperature displays a symmetry different from that dictated by the edges of the "quantum box" when the size of it becomes smaller than twice the Fermi wavelength. The inset of Figure 5 shows the interference pattern seen on a small trapezoidal island. The wavefronts are not simply parallel to the edges, but seem to originate also from the upper corner. The phase relaxation length of the surface state electrons of Cu(111) at the Fermi level and 77 K has been determined to be ≈660 Å [8]. One can, thus, assume that the surface electrons confined to these small islands scatter elastically off the potential at the Cu/Cu_3N edges several times during their lifetime. It is known that the eigenstates of a "quantum box" with hard walls always display the same symmetry than the "box". Therefore, the interference pattern of surface electrons in small island might contain information on the actual scattering properties (phase shifts, etc.) of the metal semiconductor (Cu/Cu_3N) interface.

An additional effect is clearly seen in the smallest islands. Figure 6 shows a topograph of the elongated Cu stripe at the upper half of Figure 5 (see also inset), whose width becomes progressively smaller as we move from region 1 to 3. The topographic image was measured at 300 K simultaneously with a grid of $I(V)$ spectra recorded on predetermined spots of the surface. Some selected dI/dV spectra (recorded at 300 K) are shown in the right panel of Figure 6. The spectrum recorded on the Cu_3N(111)-like regions (zone 4) of the surface show a vanishing density of states as the Fermi level is approached and indicates that the N-containing reconstruction is semiconducting, in agreement with UPS measurements on Cu_3N films that cover completely the surface [21]. This, together with the Cu band gap along ⟨111⟩ that confines the electrons perpendicularly to the surface, should confine efficiently the Cu surface state electrons within the Cu islands. When the lateral size of the confinement region becomes smaller than the Fermi wavelength of the surface state electrons (30 Å), no interference pattern would be detected. In that case, the confinement in such a small structure should shift upwards in energy the bottom of the surface state band. This is supported by the experiment.

The spectra recorded on zone 1 (31 Å wide) show the bottom of the state at the same position than in an extended Cu(111) surface (-440 ± 40 meV). The anisotropic shape of the Cu surface state is clearly seen. The bottom of the surface state band appears as an onset in the dI/dV curve. At 300 K it is much easier to pick precisely the maximum of the differential conductance than the (thermally broadened) initial rise, therefore we label the position of the surface state by the maximum in the spectra. For the extended surface the maximum occurs at −0.3 eV. It is evident from the spectra in the right panel of Figure 6 that the bottom of the state shifts upwards in energy when

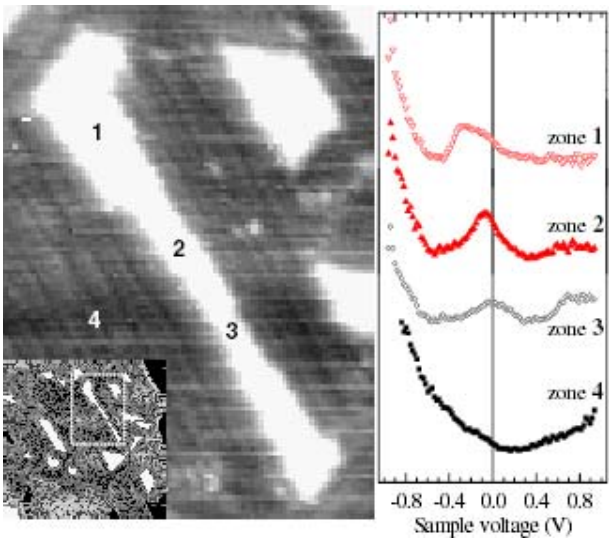

Fig. 6. The left panel shows a 16 nm × 22 nm STM topograph recorded simultaneously with a grid of 52 × 52 $I(V)$ curves. Each I-V curve contains 100 points. The current has been measured during 320 μsec in every point. The right panel shows the corresponding dI/dV versus V_s spectra taken in the regions 1−4 indicated above. The state energy shifts towards the Fermi level due to quantum confinement.

the lateral size of the Cu nanostructures becomes smaller than 22 Å (see the spectra for zone 2). The maximum of the spectrum is already at the Fermi level for stripes ≈15 Å wide (see zone 3). An upward shift by 190 meV of the surface state was previously detected in vicinal Cu (111) surfaces for terraces smaller than 25 Å [22,23] by ARUPS and STS. The shift was assigned to partial electron confinement within the terraces by the potential barriers at the steps [22,23]. For vicinal surfaces however, the physics of the confinement is complicated by the fact that the surface state is derived from the bulk band edges and the projection of the bulk band gap changes with the miscut angle. For 1D chains of Fe atoms on the surface of a SiFe(100) alloy, the surface state was observed to be 0.3 eV higher in energy than on an extended Fe(100) surface [24]. Although these authors [24] did not mention a reason for the observed shift, we ascribe it also to electron confinement in the wires.

There are several physical reasons for a Shockley surface state to shift in energy. In the first place, a modification of the potential in the first layer produced, for example, by a monolayer of foreign material would produce a shift in the energy of the bottom of the band. This has been observed for a Xe monolayer on Cu(111) [25], which shift the Cu surface state 130 meV towards the Fermi level. Similar shifts have been detected for a monolayer of Ag [26] (+220 meV) and Ni on Cu(111) [20]. Tensile strain, e.g. in Ag/Si(111) could also shift the surface state upwards in energy [27]. Notice that the effect described here is due solely to confinement and is robust enough to be detected at 300 K. It is so strong, in fact, that it involves a substantial depopulation of the surface state, which may have consequences concerning the chemical reactivity of such as small nanostructures. In effect, it has been recently proposed that the enhanced reactivity towards oxygen of the first few MLs of Cu epitaxially grown on Ru(0001) is related to the *depopulation* of the Cu surface state produced by the tensile strain of the Cu layers [28]. In that case the upward shift of the surface state for the pseudomorphic monolayer of Cu produced by the 5 per cent expansion of the lattice parameter was so large that the state was fully located above E_F.

Financial support by project BFM 2001-0174 is gratefully acknowledged.

References

1. M. Haruta, Catalysis Today **36**, 153 (1997)
2. R. Otero, A.L. Vázquez de Parga, R. Miranda, Phys. Rev. B **67**, 115401 (2002)
3. D.-A. Luh et al., Science **292**, 1131 (2001)
4. J.E. Inglesfield, Rep. Prog. Phys. **45**, 223 (1982)
5. S.D. Kevan, J. Electr. Spec. Rel. Phen. **75**, 175 (1995)
6. M.F. Crommie, C.P. Lutz, D.M. Eigler, Nature **363**, 524 (1993)
7. L. Petersen et al., Phys. Rev. B **57**, R6858 (1998)
8. L. Bürgi, H. Brune, O. Jeandupeux, K. Kern, J. Elec. Spectr. Rel. Phen. **109**, 33 (2000)
9. M.F. Crommie, C.P. Lutz, D.M. Eigler, Science **262**, 216 (1993)
10. J. Li, W.-D. Schneider, R. Berndt, S. Crampin, Phys. Rev. Lett. **80**, 3332 (1998)
11. A.L. Vázquez de Parga et al., Phys. Rev. Lett. **80**, 357 (1998)
12. L. Petersen et al., J. Elec. Spec. Rel. Phen. **109**, 97 (2000)
13. D. Fujita et al., Surface Sci. **423**, 160 (1999)
14. L. Petersen et al., Surface Sci. **443**, 154 (1999)
15. S.D. Kevan, Phys. Rev. Lett. **450**, 526 (1983)
16. J.F. Skelly et al., Surface Sci. **415**, 48 (1998)
17. S.M. Driver, D.P. Woodruff, Surf. Sci. **442**, 1 (1999)
18. V. Higgs et al., J. Elec. Spectr. Rel. Phen. **39**, 137 (1986)
19. S.L. Silva, F.M. Leibsle, Surf. Sci. **441**, L904 (1999)
20. S. Pons, P. Mallet, J.Y. Veuillen, Phys. Rev. B **64**, 193408 (2001)
21. C. Navío, J. Alvarez (private communication)
22. J.M. García et al., Appl. Phys. A **61**, 609 (1995)
23. O. Sánchez et al., Phys. Rev. B **52**, 7894 (1995)
24. A. Bidermann et al., Phys. Rev. Lett. **76**, 4179 (1996)
25. Ji-Y. Park et al., Phys. Rev. B **62**, R16341 (2000)
26. A. Bendounan et al., Surf. Sci. **496**, L43 (2002)
27. G. Neuhold, K. Horn, Phys. Rev. Lett. **78**, 1327 (1997)
28. R. Otero et al., Surface Sci. **550**, 65 (2004)